Quaternary Research
doi:10.1006/qres.2002.2370

Early to Mid-Holocene Aridity in Central Chile and the Southern Westerlies: The Laguna Aculeo Record (34°S)

Bettina Jenny[1]

Department of Physical Geography, University of Bern, Hallerstrasse 12, 3012 Bern, Switzerland

Blas L. Valero-Garcés

Pyrenean Institute of Ecology, Spanish Scientific Research Council, Apdo 202, Zaragoza 50080, Spain

Rodrigo Villa-Martínez

Laboratory of Palinology, Department of Biology, Universidad de Chile, Casilla 653, Santiago, Chile

Roberto Urrutia

Centro EULA-Chile, University of Concepción, Casilla 160-C, Concepción, Chile

Mebus Geyh

Institute for Joint Geoscientific Research, Stilleweg 2, Hanover 30655, Germany

and

Heinz Veit

Department of Physical Geography, University of Bern, Hallerstrasse 12, 3012 Bern, Switzerland

Received June 6, 2001

Central Chile (32–35°S) lies at the northern border of strong Westerly influence and thus exhibits a steep precipitation gradient. Therefore, the palaeoclimatic archives in the region are suitable for detecting past moisture changes. The study of Laguna Aculeo (33°50′S, 70°54′W) presents a multiproxy Holocene lake record including sedimentology, geochemistry, mineralogy, pollen, diatoms, and radiocarbon dating (17 dates). Results indicate an arid early to mid-Holocene period (about 9500–5700 cal yr B.P.). After 5700 cal yr B.P. effective moisture increased progressively and, around 3200 cal yr B.P., modern humid conditions were established. Numerous intercalated clastic layers reflect flood deposition during rainy winters. A fluvial unit was deposited shortly before 9000 cal yr B.P. Subsequently, flood events were absent until 5700 but have become frequent since 3200 cal yr B.P. The frequency of flood layers possibly points to weak or no El Niño activity during the early and mid-Holocene, with a subsequent increase during the late Holocene. During the early and mid-Holocene, the Westerlies were probably blocked and hence deflected southward by the subtropical high-pressure cell. Higher precipitation during the last 3200 yr seems strongly related to a weakened subtropical high-pressure cell with intensified Westerlies and possibly increased El Niño activity.

Key Words: **El Niño; South America; Holocene; mid-Holocene; diatoms; pollen; lake sediments.**

INTRODUCTION

Recently there has been a growing interest in the mid-Holocene as a period of profound environmental and climate changes and high spatial variability. Therefore, acquisition of widely distributed high-quality Holocene palaeoclimate data has been a goal within the palaeoclimate community (e.g., Steig, 1999; Sandweiss *et al.*, 1999). In the region of central Chile with a Mediterranean climate (32–35°S), which lies under the influence of the Westerly circulation belt, the mid-Holocene appears to have been an arid period as indicated by pollen (Heusser, 1983, 1990; Villagrán and Varela, 1990), marine sediment (Lamy *et al.*, 1999), and palaeosol (Veit, 1996) indicators. However, the chronology and resolution of these few records for the mid-Holocene are limited. Farther north in the Altiplano where precipitation is controlled by the tropical circulation, lake sediments from Lake Titicaca (e.g., Wirrmann and Mourguiart,

[1] To whom correspondence should be addressed. Fax: 41 (0)31 631 85 11. E-mail: jenny@giub.unibe.ch.

0033-5894/02 $35.00

1995; Cross *et al.*, 2000) and Laguna Miscanti (Valero-Garcés *et al.*, 1996) also provide evidence of a dry mid-Holocene. In contrast, only pollen from midden packs and diatoms from springs suggest that humid conditions could have occurred in limited Altiplano areas during the mid-Holocene (Betancourt *et al.*, 2000).

Here, we present a detailed multiproxy study of Laguna Aculeo (33°50′S), which supports the occurrence of a dry mid-Holocene in central Chile, with profound changes during the transition to a humid late Holocene. Central Chile (32–35°S) is situated at the northern border of the strong influence of the Westerly circulation belt (Westerlies). The precipitation gradient is especially steep in this region with high rainfall in the south (lake district) and increasingly drier conditions toward the north (Norte Chico). Consequently, palaeoclimatic archives are expected to have reacted sensitively to humidity changes. Moreover, in modern climate, increased rainfall in central Chile highly correlates with El Niño periods (Rutllant and Fuenzalida, 1991), but no data are available for the entire Holocene. In tropical and subtropical regions of South America, there are indications of changes in El Niño activity during the Holocene, although the interpretations are not in agreement, particularly for the mid-Holocene. A lake record in Ecuador (Rodbell *et al.*, 1999) indicates that El Niño was active throughout the Holocene, and deVries *et al.* (1997) and Perrier *et al.* (1994), for example, also suggest that El Niño/Southern Oscillation (ENSO) was active before 5000 yr B.P. However, archaeological and molluscan records from the coast in southern Peru (Sandweiss *et al.*, 1996, 1999) indicate that there was no El Niño activity during the mid-Holocene from about 8000 to 5000 ^{14}C yr B.P. Studies of debris flow activities in the same region (Keefer *et al.*, 1998; Fontugne *et al.*, 1999) point to minimal or no El Niño activity during the mid-Holocene. These studies propose an onset of El Niño around 5000 ^{14}C yr B.P. The record of Laguna Aculeo shows many flood events unevenly distributed, which may point to Holocene changes in ENSO activity as well.

GEOGRAPHICAL AND GEOLOGICAL CONDITIONS

The Laguna Aculeo (33°50′S, 70°54′W, elevation 350 m), with a surface of 12 km^2 and a depth of up to 6 m, is one of the largest natural lakes in the lowlands of central Chile (32–35°S). The lake has been a tourist attraction since the 1960s, and today it is a eutrophic system (Cabrera and Montecino, 1982). It lies in a tectonic basin in the coastal Cordillera (Fig. 1), and clastic input from the catchment provides a significant amount of sediments, with no inflow from the Andes. Laguna Aculeo shows high sensitivity to storm events because of the steep relief around the lake, reaching up to 2000 m in the southwest, and abundant ephemeral creeks, which enter the lake. The southeastern part of the catchment does not drain into the lake, but into the Maipo River (Fig. 1). The lake has a small outflow on the eastern side, which runs dry in summer and is rarely filled with water even in winter. No groundwater data for the lake are available. Since this outflow can be virtually neglected, water loss occurs mainly through evaporation. The catchment area consists mainly of andesites and granodiorites without carbonate-bearing rocks (Corvalán and Munizaga, 1972). The lake is surrounded by Quaternary alluvial fan deposits. The distal areas of the alluvial fans and the plains around the lake are used for agriculture. The uppermost soil horizons are often eroded, most probably due to flood splashes during the rainy winter season, and washed into the lake. Modern sediments in the central and deep areas of the lake are composed of dark-colored, massive to banded diatomaceous, organic-rich, noncarbonate muds. Littoral sediments show lighter colors, variable but low carbonate content, and macrophyte plant remains. Sand and silt occur close to the mouth of the creeks entering the lake.

Laguna Aculeo lies at the northern border of the strong Westerly influence, and the climate is Mediterranean. The summer is dry with high evaporation rates and the frontal system of the Westerlies is blocked by the very stable subtropical high-pressure cell. Winter is humid as precipitation is related to a northward shift of the Westerly storm tracks along the coast due to the northward displacement of the high-pressure cell (Aceituno, 1988). Figure 2 shows the annual precipitation distribution in the 20th century. Average annual precipitation at Laguna Aculeo is 545 mm (72-yr average). Very heavy winter rainfall in this area occurs mainly during El Niño years (e.g., Rutllant and Fuenzalida, 1991), often with precipitation higher than 1000 mm/yr at Laguna Aculeo, as shown in Figure 2. Aceituno (1988) explains how during El Niño years the temprature gradient between the tropics and the higher latitudes increases and therefore the Westerlies are strengthened with more frontal activity and rainfall. The interannual rainfall variability in this region is significantly influenced by the ENSO with warm (cold) events in the central equatorial Pacific associated with wet (dry) conditions in central Chile (Montecinos and Aceituno, 1997). Mechanisms explaining this association have to do with the weakening of the subtropical anticyclone and an increase in blocking episodes to the southwest of the continent during the negative SO phase (Rutllant and Fuenzalida, 1991). Diagnostic studies have also revealed a significant tendency for less than normal precipitation during La Niña episodes when the subtropical anticyclone is anomalously strong, thus blocking the entrance of extratropical fronts to central Chile (Montecinos and Aceituno, 1997).

METHOD

Two sediment cores, 172 and 482 cm long, were taken from the deepest part of Laguna Aculeo in 1998, using a modified Livingston 5-cm-diameter piston corer. The end of the lacustrine sequence could not be reached, because gypsum-rich indurated sediment prevented further penetration. The facies and sedimentary units were defined using lithology, organic macrorests, sedimentary structures, smear slides, and thin sections. Whole-core magnetic susceptibility was measured with a Bartington bridge

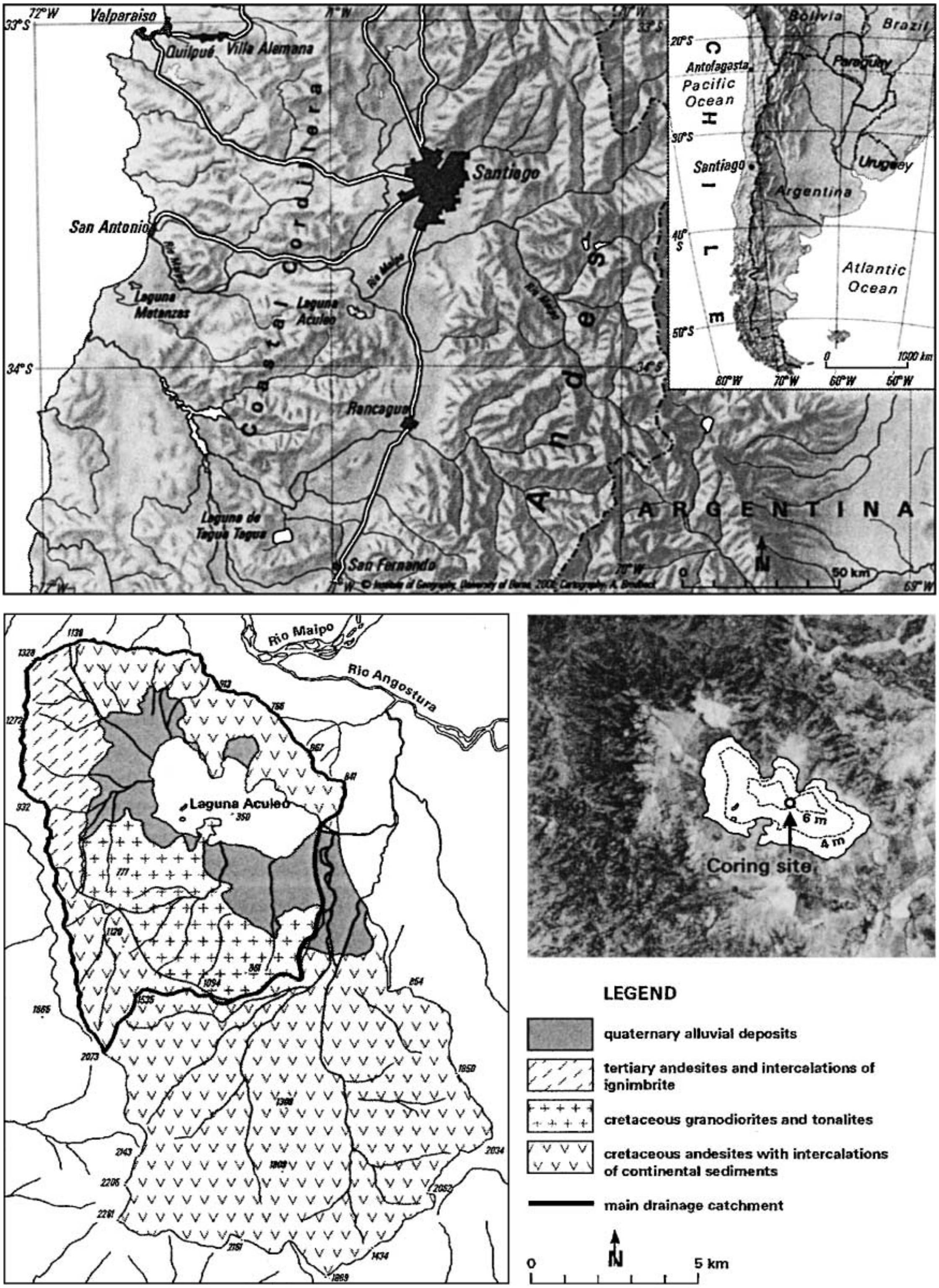

FIG. 1. Geographic and geologic setting of Laguna Aculeo. Geologic units are indicated according to Corvalán and Munizaga (1972).

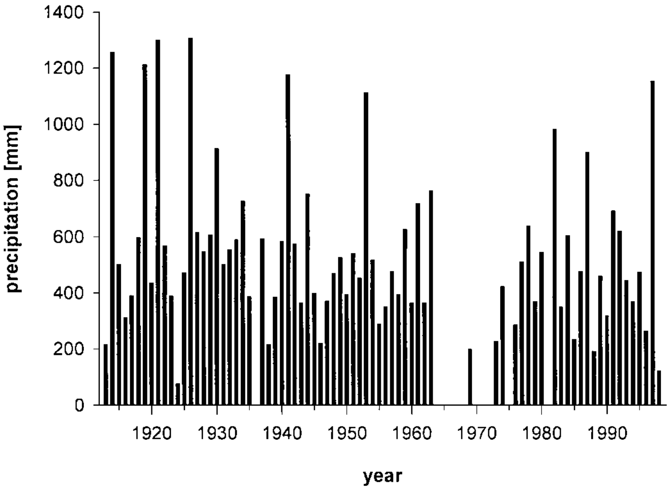

FIG. 2. Annual precipitation at Laguna Aculeo. There is a lack of data for 1936, 1964–68, 1969–72, 1975, and 1981. Precipitation data are gathered from three stations (Aculeo, Pirque, Paine) close to Laguna Aculeo. Data are provided by the Dirección General de Aguas, Chile.

at 0.5-cm intervals. Sedimentological description and magnetic susceptibility allowed a precise correlation of the cores. Inorganic and organic carbon content was measured with a CM5012 CO_2 coulometer. For the determination of major cations and trace metals, subsamples (50–200 mg) were digested in 0.3 M HNO_3 (carbonate fraction) or 3 M HNO_3 (trace metals and siliciclastic fraction), agitated for 12 h, and then measured on a Liberty ISOAX Varian ICP. Gypsum was determined by X-ray diffractometry. Additionally, for the subsequent calculation of gypsum concentration, the sulfate concentration was determined by ion chromatography after the samples had been agitated in pure water for 24 h.

For pollen analyses samples of 2–3 cm^3 were processed using potassium hydroxide, hydrofloric acid, and acetolysis (Faegri and Iversen,1989). A minimum of 300 terrestrial pollen grains were counted for each level. Approximately 100 mg of dry sediment was processed for diatom analyses after Hasle and Fryxell (1970). A minimum of 500 frustules were counted in random transects (relative abundance). Diatom classification, salinity, and life forms are discussed in Jenny *et al.* (2002). Biogenic silica concentration was calculated using the method of Mortlock and Froelich (1989).

CHRONOLOGY

To establish an accurate chronology, two independent dating methods, ^{14}C and ^{210}Pb, were applied. The age–depth relationship (Fig. 3) used in this study is based on linear interpolation. The clastic layers are removed from the age calculation because of their rapid deposition. We preferred a linear interpolation to a smoothing polynomial method because several dates are located at stratigraphic boundaries. Unsupported ^{210}Pb activity was detected to a depth of 50 cm (Fig. 3b). Concentrations of ^{210}Pb were significantly above limits of detection only in near-surface samples and at a core depth of 20–30 cm. At other depths the ^{210}Pb atmospheric deposition appears to have been largely diluted by episodes of rapid sedimentation. A mean ^{210}Pb flux to the sediments is estimated to be 48 ± 5 Bq m^{-2} yr^{-1}. More detailed information is given in Jenny *et al.* (2002). Samples from other sections were dated by ^{14}C (Table 1, Fig. 3a). To account for the southern hemisphere correction, 24 yr were subtracted (Stuiver *et al.*, 1998). The radiocarbon dates were calibrated to calendar years using the Calib 4.3 program (Stuiver and Reimer, 1993).

The organic carbon in the first 10 cm of sediment yielded a ^{14}C value of 110.3 ± 0.8 pMC, which corresponds to a modern age after 1963, suggesting no reservoir effect. In the lowest part of the core, the inorganic carbon is about 1000 yr younger than the organic matter. Considering that these sediments were deposited in an ephemeral lake system (see Results), we propose recrystallization of carbonates during the early diagenesis or formation of secondary carbonates during subsequent desiccation phases as a possible explanation for this younger age. The sedimentation rate was relatively constant between 0 and 9000 cal yr B.P. Sedimentation was faster, however, for the upper 66 cm, presumably due to eutrophication, and for the lowest part of the core where clastic input is high.

RESULTS

In the following sections, we describe the results provided by different proxies (sedimentology, geochemistry, magnetic susceptibility, pollen, and diatoms), as shown in Figures 4 and 5.

Sedimentology and Geochemistry

Sedimentary facies and structures, grain size and magnetic susceptibility, mineralogy, and bulk geochemistry provide criteria for identifying eight depositional environments in the core

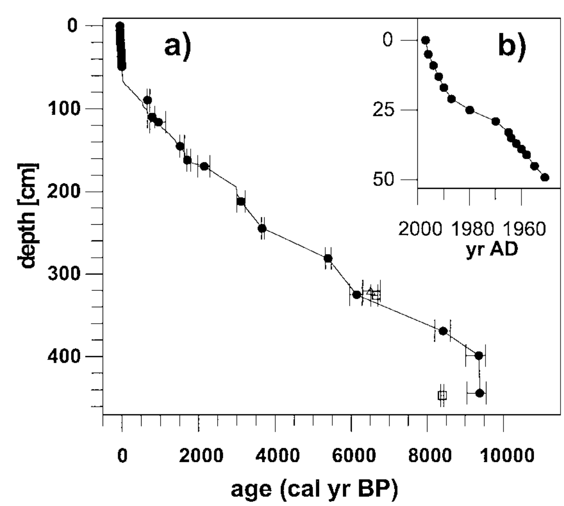

FIG. 3. Age–depth relationship. Ages are based on ^{14}C and ^{210}Pb dating (a). (b) A detailed ^{210}Pb profile. Radiocarbon dates are based on organic (dots) and inorganic carbon (squares) and are calibrated after Stuiver and Reimer (1993), including a $\pm 1\sigma$ uncertainty.

TABLE 1
Radiocarbon Dating of the Aculeo Core

Depth (cm)	Age (^{14}C yr B.P.)	Age (cal yr B.P.)	1σ max. and min. cal yr B.P.	δ^{13}C (‰ PDB)	Material	Lab code
5	>AD 1963			−17.6	OM	Hv-23487
89.5	755 ± 70	670	730–650	−24.8	OM	Ua-16877
110	920 ± 70	790	920–730	−29.6	Small wooden branch, charcoal	Ua-15089
116	1065 ± 170	950	1270–760	−24.6	OM	Hv-22728
145.5	1630 ± 60	1520	1540–1410	−28.5	Wood	NSRL-10855
162	1800 ± 40	1710	1730–1630	−15.6	Aquatic plants	NSRL-10856
169.5	2195 ± 100	2150	2330–2010	−22.9	OM	Hv-22729
212	2960 ± 50	3110	3210–3000		Charcoal, *Chenopodiaceae*	NSRL-11019
245	3450 ± 40	3660	3720–3640		Plants	NSRL-10859
281	4680 ± 50	5390	5470–5320	−25.2	*Chenopodiaceae* and *Carex*	NSRL-10857
320.5	5765 ± 220	6500	6760–6300	−24.4	OM	Hv-23496
325	5380 ± 110	6140	6280–5950	−25.8	Charcoal, fruits	Ua-15090
326	5860 ± 70	6650	6690–6550	−4.5	Inorganic carbon	Ua-16114
369	7640 ± 220	8400	8600–8180	−25.5	OM	Hv-23962
398.5	8340 ± 220	9350	9530–9010	−25.1	OM	Hv-23963
444	8390 ± 230	9380	9550–9030	−25.6	OM	Hv-23488
447	7610 ± 90	8390	8420–8340	−12.6	Inorganic carbon	Ua-16113

Note. Ua = Uppsala (AMS); NSRL = Boulder (AMS); Hv = Hanover (conventional dating), OM = organic matter; PDB, Peedee belemnite standard.

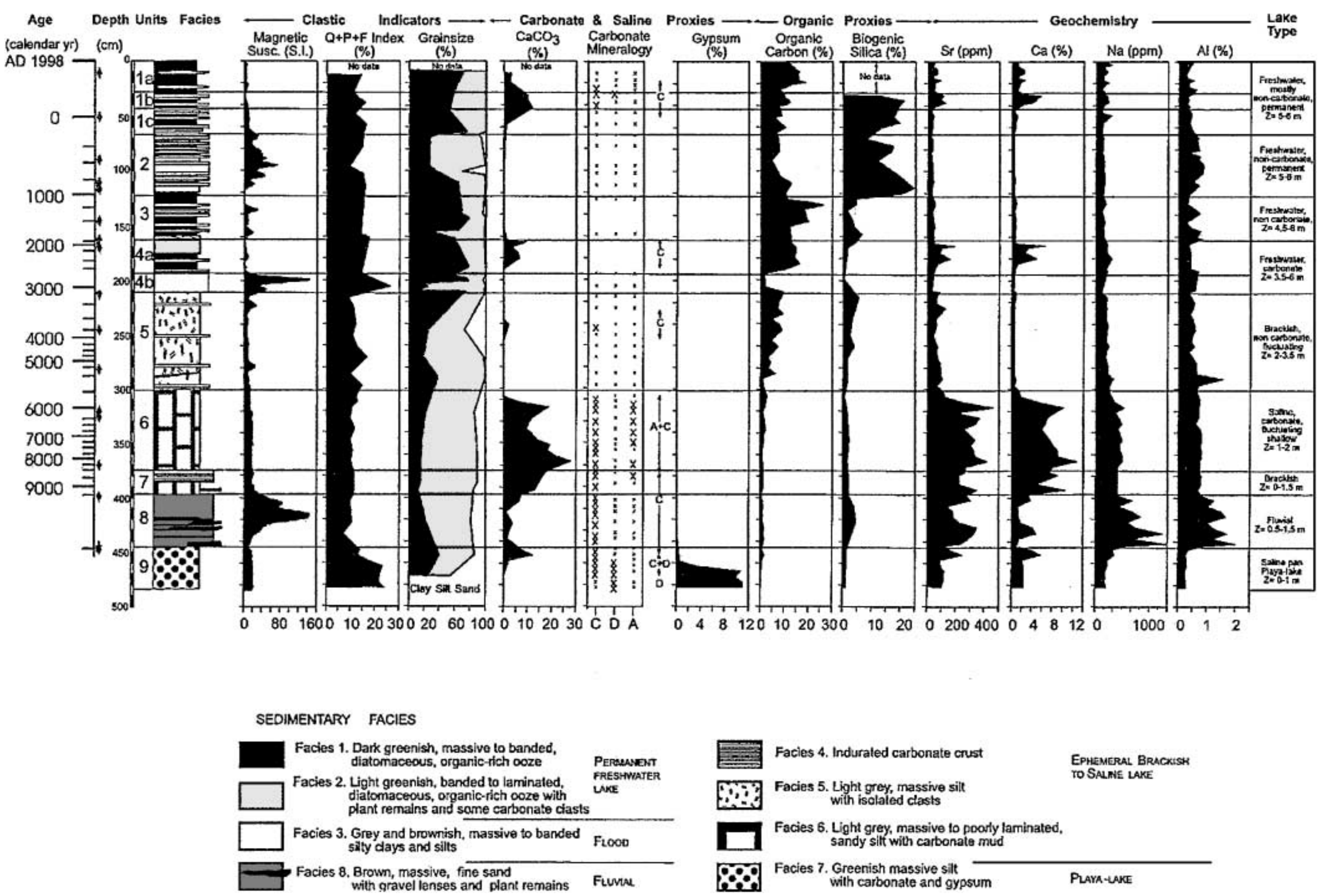

FIG. 4. Overview of the sedimentological and geochemical record. All percentage indications are in weight%. Dots beside the calibrated age scale indicate radiocarbon dates. Q = quartz, P = plagioclas, F = feldspar, C = calcite, D = dolomite, A = aragonite. X indicates presence, x indicates absence. Lake-level estimates *Z* are based on all proxies.

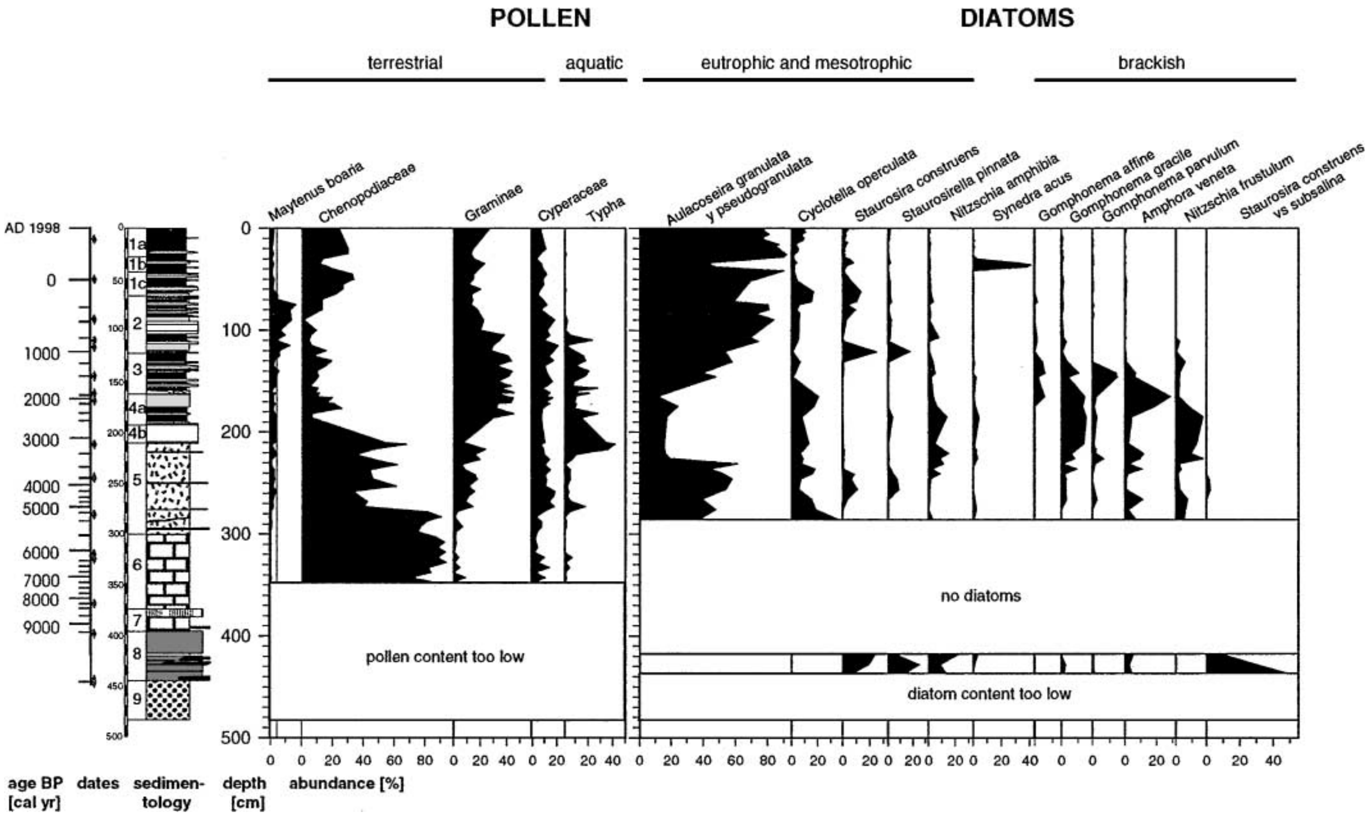

FIG. 5. Overview of main pollen and diatom taxa. Land and aquatic pollen percentages are indicated separately.

(Fig. 4). Facies 1 and 2 are interpreted as deposits in a freshwater, relatively deep lake. In Facies 1, the high concentrations of organic matter (OM) and diatoms, and the absence of carbonates, indicate a freshwater lake without significant detrital input and a lake level similar to today's or even higher. The massive character of the sediments suggests frequent oxic conditions at the lake bottom with bioturbation. This facies is similar to modern sediments deposited in the central, deeper areas of the lake. In Facies 2, the high siliciclastic content, the presence of macrophyte rests and intraclasts, and the erosive nature of the lower contacts indicate deposition during periods of increased fluvial input. Such conditions prevailed in modern littoral environments but may even reach the deepest areas of the lake during flooding episodes.

Facies 3 reflects clastic deposition during flood periods. Facies 3a is characterized by relatively high OM content derived from macrophyte remains and large amounts of clasts composed of lacustrine sediment. Both features suggest reworking of littoral sediments during floods. Finer grained Facies 3b represents deposition of suspended clastic material. Overall, Facies 3 reflects fluvial input during moderate to relatively high lake levels. Sediments from the catchment were probably mobilized during periods of extremely high rainfall. The finer particles were transported in suspension to the central area of the lake. Slow deposition resulted in graded, fining-upward layers.

Facies 4, 5, 6, and 7 are interpreted as depositions in lacustrine environments shallower than Facies 1 and 2, with fluctuating lake levels and salinity. There are no modern analogues for these facies at Laguna Aculeo. Facies 4 is a unique layer composed of carbonate clasts in a siliciclastic matrix, topped by a massive calcite-cemented horizon showing evidence of lake desiccation. Facies 5 and 6 are light gray silts with a low organic content and variable amounts of carbonate characteristic of aragonite and calcite-producing saline lakes (Facies 6) and noncarbonate shallow lakes (Facies 5). Facies 7 consists of calcite- and dolomite-bearing ($\leq 10\%$) silts with gypsum ($\leq 10\%$), indicating deposition in a playa–lake system with frequent desiccation stages. Abundant clasts suggest a reworking during short-term flooding episodes. Despite the high amount of quartz, feldspar, and plagioclases, the magnetic susceptibility is very low. Magnetic minerals may possibly have been altered due to nonoxidant conditions.

Facies 8 is coarse-grained and composed of brown, massive gravel and sands arranged in fining-upward sequences. Carbonate content, consisting only of calcite, is low, while the high aluminum and silicate content and high magnetic susceptibility parallel the increase in grain size. The coarse-grained and oxidized nature of the sediments indicate fluvial deposition in the lake basin during low lake level.

Based on the facies described, nine sedimentary units were identified (Fig. 4). An ephemeral playa lake with highly mineralized waters occurred during deposition of Unit 9. Then, an abrupt increase in river activity caused deposition of the fluvial Facies 8. The disappearance of dolomite and gypsum and the presence of calcite indicate fresher waters and probably a higher lake level than before. This unit, however, shows the highest sodium content, which is probably related to erosion of saline soils developed within the lake basin during previous desiccation periods. Afterward, the sharp decrease in Al, Na, and magnetic susceptibility, together with the increase in the carbonate concentration and related geochemical indicators (Ca, Sr), marks the end of fluvial dominance and the onset of lacustrine-dominated Unit 7. Overall, the occurrence of massive silts with gravel-size clasts and reworked deposits in Unit 7 indicates high-energy depositional conditions in the lake environment. Carbonates consisted mainly of calcite, suggesting low-mineralized waters. However, the presence of indurated carbonate horizons indicates desiccation phases. The occurrence of aragonite and the highest carbonate, Ca, and Sr contents of the core in Unit 6 indicate a brackish-saline, carbonate-producing shallow lake. The absence of indurated horizons points to a more permanent water body. The onset of Unit 5 is marked by the disappearance of carbonate and an increase in organic carbon content (Facies 5). The absence of carbonate likely indicates more dilute waters and, likely, a deeper lake.

In Unit 4, a large limnological change occurred after the deposition of a 15-cm-thick, silty layer (Unit 4b), interpreted as an intense flooding episode. Overall, Units 4–1 are characterized by finer grain size, higher OM concentration ($\leq$20%), and better developed lamination, all pointing to a higher lake level than before. Unit 4a is characterized by the alternation of an organic-rich (Facies 1) and a dominating carbonate-rich facies (Facies 2). Unit 3 is marked by the disappearance of calcite and the dominance of dark-colored, organic-rich Facies 1. A large decrease in organic carbon content and an increase in biogenic silica inaugurate Unit 2, which contains many clastic layers (Facies 3). Unit 1 shows fewer flood layers (Facies 3) and a dominance of organic-rich Facies 1.

Pollen

Figure 5 shows the main indicator pollen taxa, which are proxies for humidity and aridity. In samples of Units 7–9 (before 7000 cal yr B.P.), pollen grains were too scarce to be counted, probably due to very arid conditions. In the upper part of Unit 6, *Chenopodiaceae* (70%–90%), which are good indicators for dry conditions, clearly dominated the vegetation, while *Graminae* ($<$10%), *Cyperaceae* ($<$10%), and the aquatic species *Typha* ($<$5%) remained low. Around 5500 cal yr B.P. (lower part of Unit 5), the proportion of *Chenopodiaceae* decreased to 40%–50%, while the proportion of tree pollen (*Maytenus*) and aquatic species *Typha* and *Cyperaceae* increased slightly.

Around 3000 cal yr B.P. (beginning of Unit 4), the most dramatic change in vegetation took place. *Typha* increased rapidly to about 40%, indicating dominant aquatic conditions in the basin; shortly after, *Chenopodiaceae* diminished to about 10%, while *Graminae* increased to 40%, pointing to grassland development in the watershed. After 2000 cal yr B.P. (base of Unit 3), *Chenopodiaceae* established between 5 and 20%. Tree pollen sharply decreased at the top of Unit 2 (around 250 yr B.P.), possibly as a consequence of human deforestation of the watershed for farming. For about the last 200 yr, the proportion of *Chenopodiaceae* has risen slightly to 20–30%, while the proportions of *Graminae* and *Typha* have decreased.

Diatoms

The diatom diagram only shows the most abundant species in Laguna Aculeo. In Unit 8 (around 9500–9250 cal yr B.P.), brackish species (*Staurosira construens vs. subsalina, Gomphonema gracile, parvulum*, and *Amphora veneta*) dominated. Between $>$9000 and 5500 cal yr B.P., no diatoms were preserved, probably due to alkaline conditions in the lake. After 5500 cal yr B.P., both brackish and meso- to eutrophic species were present, but most brackish species disappeared around 1500 cal yr B.P. For the last 50 years, the species *Aulacoseira granulata, Melosira pseudogranulata*, and *Cyclotella operculata* have shown their highest abundance during the Holocene, indicating a highly eutrophic lake, which is also described by Cabrera and Montecino (1982).

DISCUSSION

Lake History

The multiproxy study of Laguna Aculeo (33°50′S) indicates profound moisture changes during the Holocene in central Chile (Figs. 4 and 5). Estimated lake-level fluctuations are shown in Figures 4 and 6. Depth estimates are based on the inferred depositional environment for each unit. Considering that the deeper lake facies only occur in relatively modern times (the upper four units corresponding to the last 2500 yr B.P.), and that Laguna Aculeo has a small outlet that controls the maximum lake level, the maximum lake depth for the whole record is about 7 m and is assigned to Facies 1. Comparison with modern sediments allows consideration of a slightly smaller depositional depth for Facies 2. Desiccation and other subaerial exposure features indicate that the lake dried out several times during deposition of the lower units. Other depositional environments are assigned intermediate depths in comparison with modern lacustrine systems.

Before 9500 cal yr B.P. (Unit 9), Laguna Aculeo was a playa–lake system with highly mineralized lake waters leading to gypsum and dolomite precipitation and to domination by brackish diatoms. Around 9500–9200 cal yr B.P. (Unit 8), fluvial gravels and sands deposited even in the inner areas of the Aculeo basin. Some areas were probably occupied by small, ephemeral lakes. After 9200 cal yr B.P. (Unit 7), shallow, ephemeral lake environments were established. The presence of an indurated layer indicates that the lake dried out afterward. Around 8500 cal yr B.P. (Unit 6), a carbonate-precipitating, more permanent saline lake was established. The high *Chenopodiaceae* and low arboreal pollen content also point to arid conditions. Laguna Aculeo became a freshwater lake around 5700 cal yr B.P. (Unit 5). The sharp decrease in *Chenopodiaceae* and the increase in arboreal

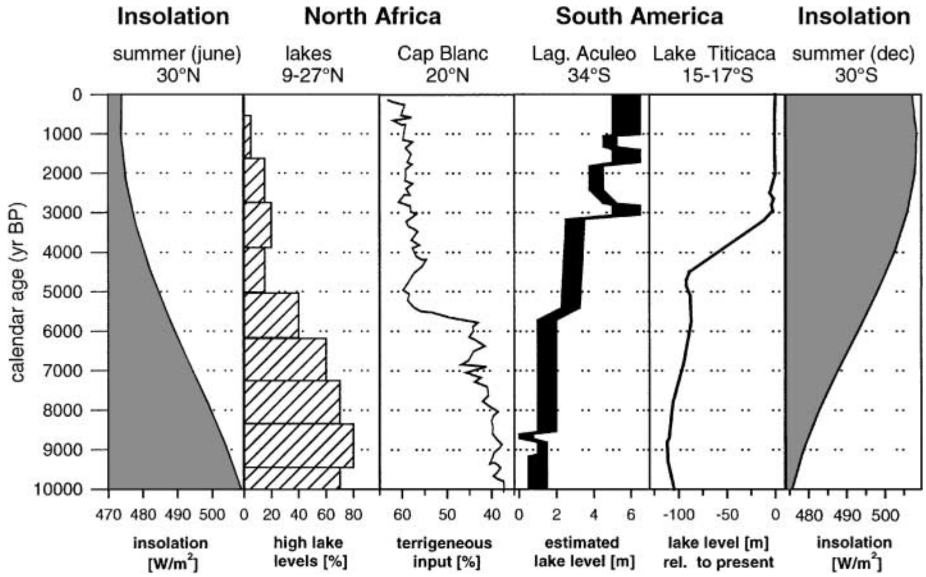

FIG. 6. Comparison of Holocene lake level of Laguna Aculeo (34°S) with records from South America and Africa. The percentage indications of high lake levels in Africa (9–27°N) are redrawn after Kutzbach and Street-Perrott (1985), the terrigenous input in marine sediments at Cape Blanc after deMenocal *et al.* (2000), the lake level of Lake Titicaca after Cross *et al.* (2000), and insolation after Berger and Loutre (1991).

(*Maytenus*) and aquatic (*Typha*) pollen taxa shortly afterward also indicate more humid conditions. Diatoms, which were completely absent during more alkaline conditions (Units 7–6), reappeared. Around 3000 cal yr B.P. (Unit 4), lake level increased after the deposition of a thick clastic layer (Unit 4b). The considerable decline in *Chenopodiaceae* and increase in *Typha* and *Graminae* also indicate more humid conditions. The higher *Typha* concentration probably reflects seasonally more stable water (Markgraf, 1989). For the last 3000 yr (Units 4–1), lake level has generally remained high, except for a period around 2000 cal yr B.P. More than 20 clastic layers in the last 3000 yr point to flooding during very rainy periods. For the last 200 yr, *Chenopodiaceae* percentages have generally increased and Maytenus percentages have decreased. These changes, however, are likely a reflection of the human impact in the region.

Palaeoclimate Implications

Precipitation in central Chile is strongly related to the Westerly circulation belt (Aceituno, 1988). The Westerlies are intensified when 1) the gradient between the South Pole and the Equator increases or 2) the southeast Pacific high-pressure cell is weakened. Under such conditions, the Westerlies are not blocked by the high-pressure cell and, therefore, more frontal systems reach farther north resulting in an increased influence of the Westerlies in central Chile (32–35°S). A weakened southeast Pacific high-pressure cell also occurs during the warm phase of ENSO (El Niño years), when the Hadley cell is weakened and abnormally warm conditions prevail in the equatorial Pacific (Montecinos *et al.*, 2000). Then, a significant tendency for positive rainfall anomalies is documented in central Chile (30–35°S). The inferred low lake levels of Laguna Aculeo during the early and mid-Holocene indicate a pronounced aridity (Fig. 6). Arid periods in central Chile generally occur when a stronger influence of the southeast Pacific high-pressure cell blocks the Westerly frontal system and deflects it farther south (Markgraf, 1989, 1998). According to Markgraf (1993), by ca. 10,000 cal yr B.P. (9000 ^{14}C yr B.P.) the storm tracks had shifted to the high latitudes in South America and the seasonal latitudinal shift, equatorward in winter and poleward in summer, probably did not develop until about 5000 cal yr B.P. (4500 ^{14}C yr B.P.). Overall, moisture availability in central Chile during the Holocene seems to have increased, while summer insolation has risen and insolation seasonality has strengthened, all reaching their maximum in the late Holocene.

According to the Aculeo record, the onset of modern humid conditions in central Chile at 34°S occurred around 3200 cal yr B.P. (Fig. 6). Dry conditions during the early to mid-Holocene and a general shift to more humid late Holocene conditions are also shown in other palaeoclimate records in the region, e.g., the pollen record of Laguna de Tagua Tagua (34°30′S, Heusser, 1990). Furthermore, Lamy *et al.* (1999) also point to arid conditions based on marine sediments (33°S) between 8000–4000 cal yr B.P. Pollen records at Quintero (31°55′S) and Quereo (32°47′S) from Villagrán and Varela (1990) and Villa-Martínez and Villagrán (1997) also suggest an arid mid-Holocene and increasing humidity around 4500 cal yr B.P. (4000 ^{14}C yr B.P.). More humid conditions in the Andes at 29°S during the late Holocene are also indicated by glacier advances (Grosjean *et al.*, 1998). At the same latitude in Argentina, the lake level of Laguna Bebedero (33°20′S) remained low between 12,000 and 5700 cal yr B.P. (Markgraf, 1989). Van Geel *et al.* (2000) even suggest that there is strong evidence for a climate change on a global scale at about 2700–2800 cal yr B.P., which was possibly caused by reduced solar energy output. The high flooding period in Laguna Aculeo occurred also around 3000 cal yr B.P.

At the Patagonian coast (41°S), where humidity is also strongly related to the Westerlies, Lamy *et al.* (2001) investigated marine sediments and propose a dry mid-Holocene from 7700 to 4000 cal yr B.P. Toward the north, on the Altiplano, moisture availability is mainly influenced by monsoonal summer rainfall. Nevertheless, Laguna Miscanti (23°45′S), for example, also provides evidence for mid-Holocene aridity with an onset of humid conditions around 4500 cal yr B.P. (4000 ^{14}C B.P.), according to Valero-Garcés *et al.* (1996). Farther north at Lake Titicaca, by 9200–8400 cal yr B.P. (8200–7700 ^{14}C yr B.P.) lake level was at least 50 m lower (Wirrmann and Mourguiart, 1995) and even 85–100 m lower by 5900 cal yr B.P. (5200 ^{14}C yr B.P.) than it is today, as shown in Figure 6 (Cross *et al.*, 2000; Seltzer *et al.*, 1998). This dry period lasted until 4000 cal yr B.P. (3600 ^{14}C yr B.P.). Conversely, only Betancourt *et al.* (2000) claim humid mid-Holocene conditions on the Chilean Altiplano based on a study of spring deposits. Their climatic interpretation of a humid mid-Holocene on the Altiplano is strongly doubted (e.g., Grosjean, 2001). In general, the mid-Holocene appears to have been a pronounced dry period not only in central Chile and Patagonia, but also on the Altiplano. The climatic forcing, however, is different. Other palaeorecords from the Southern Hemisphere also show coherency with the Aculeo record. In New Zealand, which is also strongly influenced by the Westerlies, an increase in Westerly circulation occurred at 5000 cal yr B.P., with further intensification around 3000 cal yr B.P. (Shulmeister, 1999).

As mentioned earlier, warm ENSO events provoke high rainfall in central Chile. From 1950 to 1998, for which a ^{210}Pb chronology is available, high rainfall at the Laguna Aculeo seems to correspond to flood layers. The high flood frequency periods between 1950 and 1998 occurred around A.D. 1950–1953, 1959–1966, 1978–1987, 1989–1992, 1993–1995, and 1997 (Jenny *et al.*, 2002). All years with annual precipitation above 600 mm and almost all El Niño years are represented by those periods of flooding. Therefore, at least for the last decades, clastic layers in Laguna Aculeo are probably correlated with strong El Niño years. Flood layers, deposited before 9000 cal yr B.P., were absent during the mid-Holocene until 5700 cal yr B.P. and became especially abundant after 3200 cal yr B.P.

While records in central Chile show high precipitation due to intensified Westerly activity, high rainfall in the arid coastal lowlands of Peru results from the invasion of warm air masses from the north and west during El Niño years (Aceituno, 1988). Records in the coastal area of Peru by Sandweiss *et al*. (1996) and Keefer *et al*. (1998) indicate that ENSO activity was absent or sharply reduced during the mid-Holocene and set in at approximately 5700 cal yr B.P. (5000 ^{14}C yr B.P.). In Ecuador, Rodbell *et al.* (1999) investigated lake sediments and suggest that ENSO activity was never absent during the Holocene, but that it was weak in the early Holocene. Moreover, the authors state a progressive increase in frequency, until the modern El Niño periodicity was established about 5000 cal yr B.P. Simulations by Clement *et al.* (2000) also point to weakened or suppressed ENSO activity during the mid-Holocene in the tropical Pacific region followed by a steady increase.

In many regions, ENSO may actually imply higher levels of precipitation, despite the increased variability, such as in coastal areas of northern Peru, Ecuador, and central Chile (Markgraf, 1998). Markgraf (1998) states that prior to about 5000 cal yr B.P., climatic variability was generally low and precipitation greatly reduced in central and northern Chile. The large increase in moisture at subtropical latitudes was probably related to an increased frequency of ENSO events during the late Holocene (McGlone *et al.*, 1992). According to these authors, it is likely that the strong influence of typical ENSO cycles only started around 5000 yr B.P. and was fully developed around 3000 yr B.P.

In Spain, the early Holocene seems to be the most humid period of the entire Holocene (Valero-Garcés *et al.*, 2000). In North Africa, Kutzbach and Street-Perrott (1985) show that a broad area had a generally greater effective moisture availability around 9000–6000 yr B.P. compared to today (Fig. 6). This belt extended from the western Sahara across to eastern Africa (9–27°N). In addition, a marine record off Mauritania exhibits a humid early and mid-Holocene with a low influx of aeolian material, since the Sahara was nearly completely vegetated and supported numerous lakes (deMenocal *et al.*, 2000). Around 5500 cal yr B.P., the terrigenous input increased drastically, indicating drier conditions (Fig. 6). North Africa is dominated by monsoonal rainfall during summer. DeMenocal *et al.* (2000) state that the early Holocene greening of North Africa has been linked to an intensification of the African monsoon due to earth orbital changes and that summer insolation in the Northern Hemisphere had been about 8% greater than today. During the Holocene, humidity in North Africa decreased while summer insolation diminished. For the mid-Holocene, Figure 6 shows that changes to drier conditions in North Africa were in contrast to an increasing moisture availability in central Chile (Laguna Aculeo) and on the Altiplano (Lake Titicaca). The transition period around 5000–6000 cal yr B.P. was a time of profound moisture changes over broad areas. In central Chile, northern Africa, as well as Mediterranean Spain, the general trend of Holocene moisture availability seems to parallel summer insolation, taking into account Northern and Southern Hemispheric differences. A possible explanation for an influence of insolation on moisture availability in central Chile is given by Clement *et al.* (2000). Their ENSO simulation is forced by variations in heating due to orbital variations in seasonal insolation and suggests that ENSO variability was weaker with fewer strong events during the mid-Holocene compared to the modern era. But the authors state that conclusions drawn from their simplified model must remain tentative. Since rainfall in central Chile is very high during El Niño years in modern times, this could be one possible explanation for a higher moisture availability related to insolation changes.

Overall, more definite conclusions require much more data and model–data comparison.

CONCLUSIONS

The record of Laguna Aculeo (33°50′S) provides detailed evidence for an arid early to mid-Holocene, a precipitation increase around 5700 cal yr B.P., and the onset of modern humid conditions around 3200 cal yr B.P. in central Chile (32–35°S). During the early and mid-Holocene, the southeast Pacific high-pressure cell was most probably blocking the Westerly frontal system and deflecting it farther south. During the late Holocene, which appears to be the most humid Holocene period, the Westerlies gained strength, and El Niño activity may have increased. In general, the rise in moisture availability in central Chile parallels the increase in the insolation seasonality during the Holocene. Overall, more high-resolution Holocene records in central Chile are needed for a better understanding of climate linkages in South America.

ACKNOWLEDGMENTS

This study was funded by the Swiss National Foundation (SNF-20.56908.99). We thank Daniel Ariztegui, Erika Gobet, Martin Grosjean, Philip Jeker, Urs Krähenbühl, Moritz Lehmann, Urs Gerber, Frank Oldfield, and Giancarlo Rizzoli for technical support and fruitful discussions; Caspar Ammann and Frank Lamy for constructive comments on the paper; and Andreas Brodbeck for the cartography. The help of Willi Tanner, Martin Grosjean, and Marc Begert during fieldwork is greatly appreciated. Constructive comments of Denis Wirrmann and an anonymous reviewer helped to improve the manuscript. We thank the departments of chemistry, mineralogy, and botany (University of Bern) and limnogeology (ETH Zurich) for lab facilities, and the University of Colorado INSTAAR-Laboratory (NSF-ATM-9809285) for radiocarbon preparation (Fondecyt-2990012).

REFERENCES

Aceituno, P. (1988). On the functioning of the Southern Oscillation in the South American sector. Part 1. Surface climate. *Monthly Weather Review* **116,** 505–524.

Berger, A., and Loutre, M. F. (1991). Insolation values for the climate of the last 10 million years. *Quaternary Science Reviews* **10,** 297–317.

Betancourt, J. L., Latorre, C., Rech, J. A., Quade, J., and Rylander, K. A. (2000). A 22,000-year record of monsoonal precipitation from Northern Chile's Atacama desert. *Science* **289,** 1542–1546.

Cabrera, S., and Montecino, V. (1982). Eutrophy of Lake Aculeo, Chile. *Plant and Soil* **67,** 377–387.

Clement, A. C., Seager, R., and Cane, M. A. (2000). Suppression of El Niño during the mid-Holocene by changes in the Earth's orbit. *Palaeoceanography* **15,** 731–737.

Corvalán, J., and Munizaga, F. (1972). Edades radiometricas de rocas intrusivas y metamorficas de la Hoja Valparaíso—San Antonio. Chile, Instituto de Investigaciones Geologicas. [In Spanish]

Cross, S. L., Baker, P. A., Seltzer, G. O., Fritz, S. C., and Dunbar, R. B. (2000). A new estimate of the Holocene lowstand level of Lake Titicaca, central Andes, and implications for tropical palaeohydrology. *The Holocene* **10,** 21–32.

deMenocal, P., Ortiz, J., Guilderson, T., Adkins, J., Sarnthein, M., Baker, L., and Yarusinsky, M. (2000). Abrupt onset and termination of the African Humid period: Rapid climate responses to gradual insolation forcing. *Quaternary Science Reviews* **19,** 347–361.

deVries, T. J., Ortlieb, L., Diaz, A., Wells, L., Hillaire, M., Wells, L. E., Jay, S., Sandweiss, D. H., Richardson, J. B., III, Reitz, E. J., Rollins, H. B., and Maasch, K. A. (1997). Determining the early history of El Niño. *Science* **276,** 965–967.

Faegri, K., and Iversen, J. (1989). "Textbook of Pollen Analysis." Amsterdam, Balkena.

Fontugne, M., Usselmann, P., Lavallée, D., Julien, M., and Hatté, C. (1999). El Niño variability in the coastal desert of Southern Peru during the mid-Holocene. *Quaternary Research* **52,** 171–179, doi:10.1006/qres.1999.2059.

Grosjean, M. (2001). Mid-Holocene climate in the South-Central Andes: Humid or dry? *Science* **292,** 2391.

Grosjean, M., Geyh, M. A., Messerli, B., Schreier, H., and Veit, H. (1998). A late-Holocene (<2600 B.P.) glacial advance in the south-central Andes (29°), northern Chile. *The Holocene* **8,** 473–479.

Hasle, G., and Fryxell, G. (1970). Diatoms: Cleaning and mounting for light and electron microscopy. *Transactions of American Microscopy Society* **89,** 469–474.

Heusser, C. J. (1983). Quaternary pollen record from Laguna de Tagua Tagua, Chile. *Science* **219,** 1429–1432.

Heusser, C. J. (1990). Ice age vegetation and climate of subtropical Chile. *Palaeogeography, Palaeoclimatology, Palaeoecology* **80,** 107–127.

Jenny, B., Valero-Garcés, B. L., Urrutia, R., Kelts, K., Veit, H., and Geyh, M. (2002). Moisture changes and fluctuations of the Westerlies in Mediterranean Central Chile during the last 2000 years: The Laguna Aculeo record (33°50′S). *Quaternary International* **87,** 3–18.

Keefer, D. K., deFrance, S. D., Moseley, M. E., Richardson, J. B., III, Satterlee, D. R., and Day-Lewis, A. (1998). Early maritime economy and El Niño events at Quebrada Tacahuay, Peru. *Science* **281,** 1833–1835.

Kutzbach, J. E., and Street-Perrott, F. A. (1985). Milankovitch forcing of fluctuations in the level of tropical lakes from 18 to 0 kyr B.P. *Nature* **317,** 130–134.

Lamy, F., Hebbeln, D., and Wefer, G. (1999). High-resolution marine record of climatic change in mid-latitude Chile during the last 28,000 years based on terrigenous sediment parameters. *Quaternary Research* **51,** 83–93.

Lamy, F., Hebbeln, D., Roehl, U., and Wefer, G. (2001). Holocene rainfall variability in southern Chile: A marine record of latitudinal shifts of the Southern Westerlies. *Earth and Planetary Science Letters* **185,** 369–382, doi:10.1006/qres.1998.2010.

Markgraf, V. (1989). Palaeoclimates in central and south America since 18,000 B.P. based on pollen and lake-level records. *Quaternary Science Reviews* **8,** 1–24.

Markgraf, V. (1993). Paleoenvironments and paleoclimates in Tierra del Fuego and southernmost Patagonia, South America. *Palaeogeography, Palaeoclimatology, Palaeoecology* **102,** 53–68.

Markgraf, V. (1998). Past climates of South America. *In* "Climates of the Southern Continents: Present, Past and Future" (J. E. Hobbs, J. A. Lindesay, and H. A. Bridgman, Eds.), pp. 249–264. Wiley, Chichester, UK.

McGlone, M. S., Kershaw, A. P., and Margraf, V. (1992). El Niño/Southern Oscillation climatic variability in Australasian and South American paleoenvironmental records. *In* "El Niño: Historical and Paleoclimatic Aspects of the Southern Oscillation" (H. Diaz and V. Markgraf, Eds.), pp. 435–462. Cambridge Univ. Press, Cambridge, UK.

Montecinos, A., and Aceituno, P. (1997). Rainfall prediction for the austral winter in Central Chile based on a CCA forecast and a Niño 3 analog evolution approach. *Experimental Long-Lead Forecast Bulletins*, June 1997.

Montecinos, A., Díaz, A., and Aceituno, P. (2000). Seasonal diagnostic and predictability of rainfall in subtropical South America based on tropical Pacific SST. *Journal of Climate* **13,** 746–758.

Mortlock, R. A., and Froelich, P. N. (1989). A simple method for the rapid determination of biogenic opal in pelagic marine sediments. *Deep-Sea Research* **36,** 1415–1426.

Perrier, C., Hillaire-Marcel, C., and Ortlieb, L. (1994). Littoral paleogeography and isotopic record ^{13}C, ^{18}O of El Niño events in modern and holocene mollusk shells from NW Peru. *Geographie Physique et Quaternaire* **48,** 23–38.

Rodbell, D. T., Seltzer, G. O., Anderson, D. M., Abbott, M. B., Enfield, D. B., and Newman, J. H. (1999). A ∼15,000-year record of El Niño-driven alluviation in southwestern Ecuador. *Science* **283,** 516–520.

Rutllant, J., and Fuenzalida, H. (1991). Synoptic aspects of the central Chile rainfall variability associated with the Southern Oscillation. *International Journal of Climatology* **11,** 63–76.

Sandweiss, D. H., Richardson, J. B., III, Reitz, E. J., Rollins, H. B., and Maasch, K. A. (1996). Geoarchaeological evidence from Peru for a 5000 years B.P. onset of El Niño. *Science* **273,** 1531–1533.

Sandweiss, D. H., Maasch, K. A., and Anderson, D. G. (1999). Transitions in the mid-Holocene. *Science* **283,** 499–500.

Seltzer, G. O., Baker, P., Cross, S., Dunbar, R., and Fritz, S. (1998). High-resolution seismic reflection profiles from Lake Titicaca, Peru-Bolivia: Evidence for Holocene aridity in the tropical Andes. *Geology* **26,** 167–170.

Shulmeister, J. (1999). Australasian evidence for mid-holocene climate change implies precessional control of Walker Circulation in the Pacific. *Quaternary International* **57/58,** 81–91.

Steig, E. J. (1999). Mid-Holocene climate change. *Science* **286,** 1485–1487.

Stuiver, M., and Reimer, P. J. (1993). Extended ^{14}C database and revised CALIB radiocarbon calibration program. *Radiocarbon* **35,** 215–230.

Stuiver, M., Reimer, P. J., Bard, E., Beck, J. W., Burr, G. S., Hughen, K. A., Kromer, B., McCormac, F. G., van der Plicht, J., and Spurk, M. (1998). INTCAL98 Radiocarbon age calibration 24,000-0 cal B.P. *Radiocarbon* **40,** 1041–1083.

Valero-Garcés, B. L., Grosjean, M., Schwalb, A., Geyh, M., Messerli, B., and Kelts, K. (1996). Limnogeology of Laguna Miscanti: Evidence for mid to late Holocene moisture changes in the Atacama Altiplano (northern Chile). *Journal of Paleolimnology* **16,** 1–21.

Valero-Garcés, B. L., González-Sampériz, P., Delgado-Huertas, A., Navas, A., Machín, J., and Kelts, K. (2000). Lateglacial and Late Holocene environmental and vegetational change in Salada Mediana, central Ebro Basin, Spain. *Quaternary International* **73–74,** 29–46.

van Geel, B., Heusser, C. J., Renssen, H., and Schuurmans, C. J. E. (2000). Climatic change in Chile at around 2700 B.P. and global evidence for solar forcing: A hypothesis. *The Holocene* **10,** 659–664.

Veit, H. (1996). Southern Westerlies during the Holocene deduced from geomorphological and pedological studies in the Norte Chico, Northern Chile (27–33°C). *Palaeogeography, Palaeclimatology, Palaeoecology* **123,** 107–119.

Villa-Martínez, R., and Villagrán, C. (1997). Historia de la vegetación de bosques pantanosos de la costa de Chile central durante el Holoceno medio y tardío. *Revista Chilena de Historia Natural* **70,** 391–401. [In Spanish]

Villagrán, C., and Varela, J. (1990). Palynological evidence for increased aridity on the Central Chilean coast during the Holocene. *Quaternary Research* **34,** 198–207.

Wirrmann, D., and Mourguiart, P. (1995). Late quaternary spatio-temporal limnological variation in the Altiplano of Bolivia and Peru. *Quaternary Research* **43,** 344–354. doi: 10.1006/qres.1995.1040.